JACS
JOURNAL OF THE AMERICAN CHEMICAL SOCIETY
Article
pubs.acs.org/JACS

Electronic Structure and Excited-State Dynamics of the Molecular Triads: *trans*-$M_2(T^iPB)_2[O_2CC_6H_5\text{-}\eta^6\text{-}Cr(CO)_3]_2$, Where M = Mo or W, and T^iPB = 2,4,6-triisopropylbenzoate

Samantha E. Brown-Xu, Malcolm H. Chisholm,* Christopher B. Durr, Terry L. Gustafson, Vesal Naseri, and Thomas F. Spilker

Department of Chemistry and Biochemistry, The Ohio State University, Columbus, Ohio 43210, United States

Supporting Information

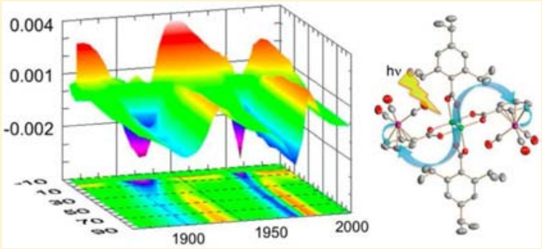

ABSTRACT: From the reactions between $M_2(T^iPB)_4$ and $HO_2CC_6H_5$-η^6-$Cr(CO)_3$ (2 equiv), the title compounds *trans*-$M_2(T^iPB)_2[O_2CC_6H_5\text{-}\eta^6\text{-}Cr(CO)_3]_2$, where M = Mo or W, and T^iPB = 2,4,6-triisopropylbenzoate have been prepared and characterized. Compound **I** (M = Mo) was characterized by a single crystal X-ray structural determination which revealed a centrosymmetric MoMo quadruply bonded molecule. Compound **I** is red and the tungsten complex **II** is blue as a result of intense metal-to-ligand charge transfer (MLCT), which is principally $M_2\delta$ to benzoate π^* with some chromium t_{2g} participation, according to calculations employing density functional theory. Compound **I** shows dual emission from S_1 and T_1 states that are assigned ^{1}MLCT and ^{3} MoMo$\delta\delta^*$, respectively. Both complexes have been studied by time-resolved infrared spectroscopy (TRIR) in the region of the carbonyl stretching frequency. Compound **II** displays a shift of ν(CO) to lower energy in both the ^{1}MLCT and ^{3}MLCT states in THF, while **I** in CH_2Cl_2 shows ν(CO) bands shifted to both higher and lower energy. We attribute the shift to higher energy seen for **I** to a Cr t_{2g} to benzoate π^* transition which mixes with the $Mo_2\delta$ to benzoate charge transfer upon excitation at 514 nm. In THF compound **I** undergoes a reversible photodissociation, potentially due to CO loss. Based on the TRIR of the carbonyl vibrations, it is proposed that the MLCT states are delocalized over both benzoate $Cr(CO)_3$ groups, as supported by calculations.

1. INTRODUCTION

Most photophysical studies of MM quadruply bonded complexes have focused on the singlet δ to δ^* transition and its weak emissive state.[1,2] The introduction of conjugated carboxylate ligands at the M_2 quadruply bonded center introduces an intense $M_2\delta$ to carboxylate π^* transition, which typically obscures observation of the $^1(\delta \to \delta^*)$ transition. Our interest in these metal-to-ligand charge transfer (MLCT) states was piqued when we discovered that the ^{1}MLCT states were relatively long-lived (approximately picoseconds) and the triplet states could be either ^{3}MLCT or ^{3}MM$\delta\delta^*$.[3−5] The lifetimes of these S_1 and T_1 states allow investigation of the excited-state dynamics in the MLCT states.[6,7] The introduction of IR reporter groups, such as C≡N and C≡C, allows the charge location to be probed with time, and we have recently reported on MLCT states that were delocalized or localized as a function of the nature of the metal and the ligands.[8]

From these previous studies, a wealth of knowledge has been accumulated concerning photophysical properties of systems with π-conjugated ligands. One area still open for exploration, however, is the attachment of secondary transition-metal units to form molecular triads. In one instance, a ditungsten complex was synthesized containing *trans*-ethynyl ferrocenyl groups; though it was found there was no electronic communication between the iron centers and excited state, data was not collected.[9] For the present spectroscopic investigations, metal carbonyl complexes are quite attractive due to the high oscillator strength of ν(CO) as well as favorable positioning of the carbonyl peaks in the IR region. The presence of additional t_{2g} orbitals also offers the potential for mixing with the $M_2\delta$ orbital, thereby altering the photophysical properties significantly.

Numerous complexes with chromium, molybdenum, and rhenium carbonyl units bound to π-ligands have warranted time-resolved spectroscopic investigations for their interesting reactions with light, including photoinduced isomerization, electron transfer, and ligand dissociation.[10−23] In particular, George and co-workers have examined several (η^6-arene)Cr-$(CO)_3$ half-sandwich complexes which undergo carbonyl dissociation following excitation of a metal-to-arene charge transfer transition.[24−27] Modification of the arene group was seen to modulate the efficiency of CO loss from the complex and even lead to a haptotropic shift in certain cases.[27,28] These in-depth studies afford us an excellent reference point for examining the influence of $M_2\delta$-to-ligand charge transfer on this organometallic fragment. Herein, we describe our preparation and characterization of the title compounds **I** (M = Mo) and **II**

Received: October 29, 2012
Published: November 29, 2012

dx.doi.org/10.1021/ja310651y | *J. Am. Chem. Soc.* 2012, 134, 20820−20826

(M = W) that bear *trans*-benzoate chromium tricarbonyl moieties.

2. RESULTS AND DISCUSSION

2.1. Synthesis. The new compounds were prepared according to the carboxylate exchange reaction shown in Scheme 1 (M = Mo or W and T^{i}PB = 2,4,6-triisopropylbenzoate).

Scheme 1. Reaction to Form Compounds I and II (M = Mo or W)

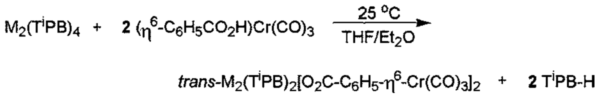

The reactions proceed with a sharp color change from the yellow-orange $M_2(T^iPB)_4$ complexes to red for **I** or blue for **II**. The new compounds are air and moisture sensitive, soluble in THF, DMSO, CH_2Cl_2, and CH_3CN and sparingly soluble in toluene and benzene. The chromium tricarbonyl benzoic acid was prepared by a modified procedure based upon literature precedent.[29] Details are reported in the experimental section along with other characterization data. Crystalline materials were prepared from cooling concentrated benzene solutions.

2.2. Single Crystal and Molecular Structure of *trans*-$Mo_2(T^iPB)_2[O_2CC_6H_5\text{-}\eta^6\text{-}Cr(CO)_3]_2$ (I). In the space group $P\bar{1}$ there are three Mo_2 units with their attendant ligands and several benzene molecules. Each molecule has a center of inversion and lacks any donor solvent coordinated along the MM axis. An ORTEP drawing of one molecule is shown in Figure 1. This view clearly emphasizes the *trans*-$(\eta^6\text{-}C_6H_5CO_2)$-$Cr(CO)_3$ units that are related by the center of inversion and shows that the C_6 aromatic plane of the T^{i}PB ligands is turned out of conjugation with its CO_2 group. The planar arrangement of the *trans*-C_6H_5-CO_2 units is indicative of extensive Lπ-$M_2\delta$-Lπ conjugation as has been seen before.[3,30]

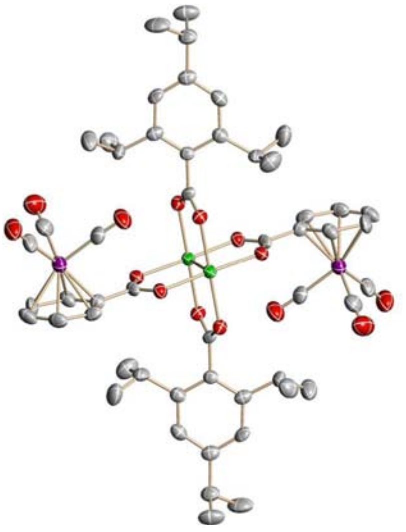

Figure 1. Thermal ellipsoid plot of **I** shown at 50% probability. One of three molecules of the unit cell is shown, and hydrogen atoms and disorder and lattice solvent are omitted for clarity. (Mo = Green, Cr = Violet, O = Scarlet, C = Gray).

The average Mo–Mo distance is 2.01(1) Å, and the metric parameters associated with the central $Mo_2(O_2C)_4$ core are unexceptional when compared with other $Mo_2(O_2CR)_4$ compounds. The Cr···C_6 centroid distance is 1.70 Å (average), which is also rather typical for arene-$Cr(CO)_3$ distances.[31] Full structural data are given in the Supporting Information.

2.3. Ground-State Infrared Spectra. The new compounds showed the expected carbonyl stretching frequencies associated with the $(\eta^6\text{-}C_6H_5CO_2)Cr(CO)_3$ units having virtual C_{3v} symmetry, namely the IR active 'A' and 'E' bands: 1977 and 1908 cm^{-1} (**I**) and 1971 and 1903 cm^{-1} (**II**) (Figure 2). These may be compared with the previously characterized chromium tricarbonyl benzoate ester $(\eta^6\text{-}C_6H_5CO_2Me)Cr(CO)_3$ that exhibits A and E modes at 1992 and 1929 cm^{-1}, respectively.[27] Both **I** and **II** have lower ν(CO) values, indicative of the enhanced backbonding from the $M_2\delta$ to the benzoate π^* orbitals, which in turn enhances the chromium t_{2g} to CO π^* backbonding. Previous studies showed that in a series of $(C_6H_5X)Cr(CO)_3$ complexes, the values of ν(CO) correlate with the electron-donating or -withdrawing properties of the substituent X.[24]

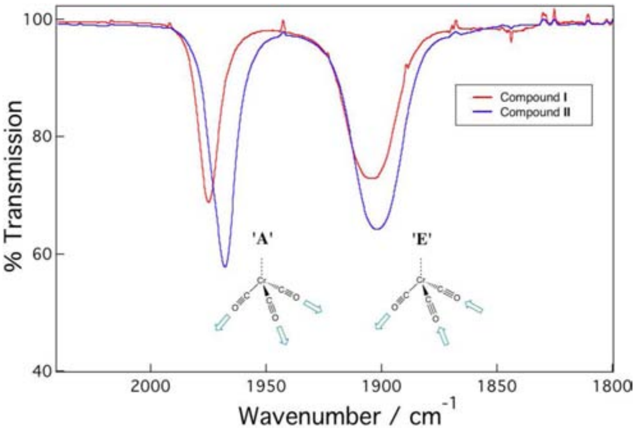

Figure 2. Ground-state infrared spectra of **I** (red) and **II** (blue) in THF.

2.4. Electronic Structure Calculations. In order to aid in an interpretation of the spectroscopic data, we have employed calculations based on density functional theory (DFT) and time-dependent DFT (TD-DFT) on model compounds where formate substitutes for T^{i}PB (M = Mo, **I′**; W, **II′**) . This saves on computational time and resources and is a reasonable approximation since the aromatic rings of the T^{i}PB ligands are not in significant conjugation with the $M_2\delta$ orbital. As a further consideration, we also examined the electronic structure of the molecules *trans*-$M_2(O_2CH)_2(O_2CPh)_2$ in D_{2h} symmetry. This allows insight into the influence of the $Cr(CO)_3$ unit attached to the benzoate ligands. In the case of the calculations on the model compounds **I′** and **II′**, the $Cr(CO)_3$ units were unconstrained, and the calculation adopted a C_i symmetry.

The frontier molecular orbital energy level diagram comparing the *trans*-benzoate and *trans*-benzoate chromium tricarbonyl model compounds is shown in Figure 3. Also shown are GaussView representations of the HOMO, LUMO, and LUMO+1. We see here that the introduction of the $Cr(CO)_3$ unit has a stabilizing influence on the HOMO by ~0.3 eV and also lowers the ligand-based π^* orbitals, which for M = Mo are the in-phase benzoate π^* (LUMO+1) and the out-of-phase

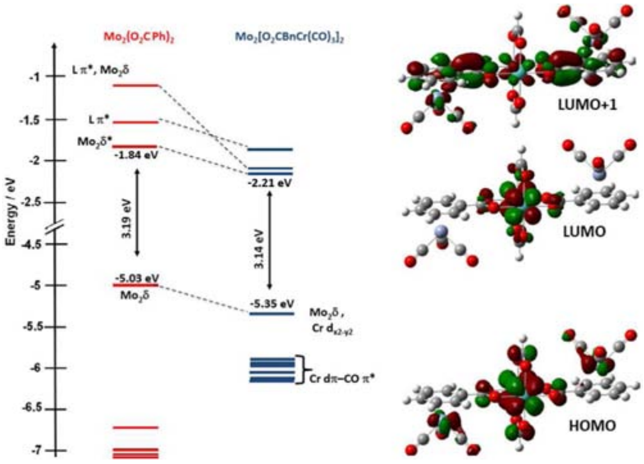

Figure 3. Energy diagram of compound **I′** (blue) and its nonmetalated counterpart (red) with GaussView representations of the frontier molecular orbitals of **I′**.

benzoate π^* (LUMO+2). The HOMO is principally a $Mo_2\delta$ orbital with some carboxylate and chromium t_{2g} mixing.

For **I′** the LUMO is the $M_2\delta^*$ orbital, but for **II′**, the LUMO and LUMO+1 are the benzoate in-phase and out-of-phase π^* combinations, while the $M_2\delta^*$ is LUMO+2. This relative ordering arises because the $W_2\delta$ orbital is ~0.5 eV higher in energy relative to its counterpart. The frontier MO diagram for the model tungsten complex is shown in the Figure S1. The results of the TD-DFT calculated predictions of electronic transitions for the neutral model compounds are noted in the following section.

The TD-DFT calculations on **I′** indicate the lowest energy transition is primarily HOMO → LUMO+1, however there is also a significant admixture of $Cr_{d\pi}$ to benzoate π^* character in this transition. For **II′**, the lowest energy transition is purely HOMO → LUMO since there is less overlap between the Cr t_{2g} and $W_2\delta$ orbitals. Transitions localized on the organometallic unit occur at higher energies, with $Cr_{d\pi}$→benzoate π^* and $Cr_{d\pi}$→CO π^* MLCT states near 400 and 300 nm, respectively.

Calculations on the lowest energy triplet states of the model compounds indicate that for molybdenum the two singly occupied orbitals have $Mo_2\delta$ + Cr t_{2g} and $Mo_2\delta^*$ character. Furthermore, the calculations predict that the carbonyl stretching frequencies will move to higher energy relative to the ground state by ~10 cm^{-1}. Calculations performed on anions of the model compounds **I′** and **II′** which have a singly occupied in-phase benzoate π^* orbital display a marked effect on the $Cr(CO)_3$ unit and predict a shift of the $\nu(CO)$ stretches by ~50 cm^{-1} to lower energy. The calculations recognize that the symmetry is reduced from C_{3v} in $(C_6H_6)Cr(CO)_3$ and so predict 3 IR active bands that formally represent the A and E bands in C_{3v} symmetry. Thus the calculations have two IR bands derived from the E mode, while for compounds **I** and **II** the resolution is not sufficient to reveal the removal of the degeneracy. Finally, we have calculated the electronic structure and vibrational spectra of $(\eta^6\text{-}C_6H_5CO_2H)Cr(CO)_3$ and its anion. Notably, the frequency of the ‘A’ carbonyl stretching mode decreases from 2070 to 2000 cm^{-1} and the ‘E’ mode from 1944 to 1852 cm^{-1} or on average ~80 cm^{-1} (Table 1).

Table 1. Comparison of ν(CO) Wavenumbers Calculated for Neutral and Anionic Compounds

	$(\eta^6\text{-}C_6H_5COOH)Cr(CO)_3$		**I′**		**II′**	
	‘A’	‘E’	‘A’	‘E’	‘A’	‘E’
neutral	1990	1947, 1941	1983	1939, 1935	1978	1937, 1931
anion	1920	1859, 1845	1930	1891, 1884	1930	1885, 1883
$\Delta\nu$(CO) (avg)	−70	−92	−53	−50	−48	−50

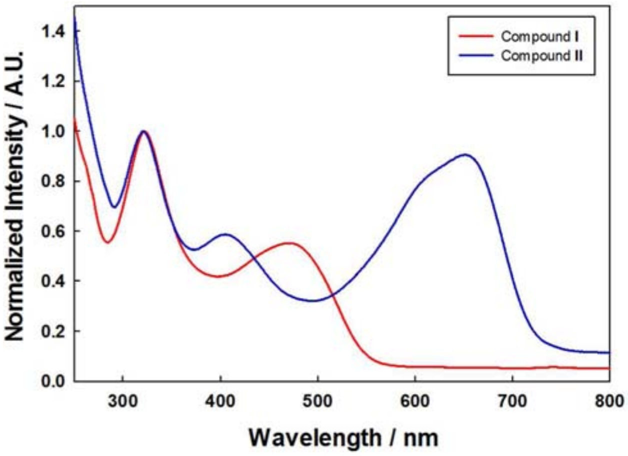

Figure 4. Electronic absorption spectra of compounds **I** (red) and **II** (blue) at room temperature in THF.

2.5. Electronic Absorption Spectra.

The electronic absorption spectra of the compounds **I** and **II** in THF are compared in Figure 4. The intense red (**I**) and blue (**II**) colors arise from the fully allowed metal-to-ligand (benzoate) charge transfer transitions. The lower energy and more intense ^{1}MLCT band associated with the tungsten complex are as expected due to the higher relative energy of the $W_2\delta$ orbital relative to its $Mo_2\delta$ counterpart. Also, for tungsten compound **II** we see an absorption at ~400 nm which is assignable to the $W_2\delta$ to T^iPB CO_2 π^* orbitals. For M = Mo, the $Mo_2\delta$ to T^iPB CO_2 π^* transition is masked by the higher energy Cr $t_{2g}{}^6$ to CO π^* transition which falls at ~320 nm for both compounds.

The observed and calculated spectra for the molybdenum complex are in relatively good agreement, especially considering the calculated spectra were for the model compounds, where formate substitutes for T^iPB and also refer to the gas phase rather than in THF solvent. The calculations for the tungsten complex are in qualitative agreement though as seen before the observed lowest energy ^{1}MLCT band occurs at lower energy than that calculated. This we suggest arises because of the greater spin−orbit mixing of the heavier 5d element for which the calculations do not adequately accommodate.

2.6. Steady-State Emission Spectra.

Compound **I** shows weak emission from its S_1 state at ~625 nm (Figure S2) and a phosphorescence at ~1100 nm with vibronic features that correlate roughly with ν(MoMo) ~400 cm^{-1} (Figure S2). This is consistent with the phosphorescence arising from the ^{3}MoMo$\delta\delta^*$ state, as has been seen for related $Mo_2(O_2CR)_4$ compounds.[7] It is also consistent with the calculations on the model compound.

The tungsten complex **II** also showed weak emission from the ^{1}MLCT state that unfortunately arose close to the limits of the two spectrometers, namely ~900 nm, which prevented collection of the spectrum. No detectable phosphorescence was observed, and the triplet state likely undergoes nonradiative decay to the ground state.

2.7. Time-Resolved Spectroscopic Studies. Both compounds have been examined by transient absorption (TA) and time-resolved infrared (TRIR) studies. TA spectroscopy has allowed us to determine the lifetimes of the singlet and triplet states, and the former have been confirmed by the TRIR femtosecond studies. For molybdenum the S_1 and T_1 states have lifetimes of 18 ps and 24 μs in CH_2Cl_2 and THF, respectively (Figure S3). For compound **II** the lifetime of the S_1 state in THF is 1.5 ps and that of the T_1 state falls between 3 and 10 ns (Figure S4). These S_1 and T_1 lifetimes are comparable to many other M_2-carboxylate complexes studied previously.[32]

The focus of the TRIR work was to examine the charge localization in the excited states and the effects of metal orbital mixing in the triad. The $Cr(CO)_3$ moieties are readily employed as reporter groups due to the high oscillator strength of $\nu(CO)$ and since much work on arene $Cr(CO)_3$ complexes has been performed previously. However, during our initial examination of the TRIR spectra of compound **I** in THF, unexpected and complex behavior was observed. This was not the case for the tungsten complex nor for compound **I** in the "noncoordinating" solvent CH_2Cl_2.

Beginning with the examination of compound **II**, the fs-TRIR spectra for the tungsten complex in THF following 675 nm excitation are shown in Figure 5. The spectra reveal the ground-state bleaches at 1970 and 1900 cm^{-1} together with broad exited-state features, which are shifted to lower energy at 1935 and 1875 cm^{-1}. These $\nu(CO)$ vibrations in the ^{1}MLCT state cool and decay within ~2 ps, and bands due to the longer-lived triplet state at 1930 and 1855 cm^{-1} remain. Weaker peaks located in higher energy from the ground state at 1980 and 1915(sh) cm^{-1} also become apparent and are attributed to some degree of involvement of the Cr t_{2g} orbitals in this state, which will be elaborated further in the discussion below.

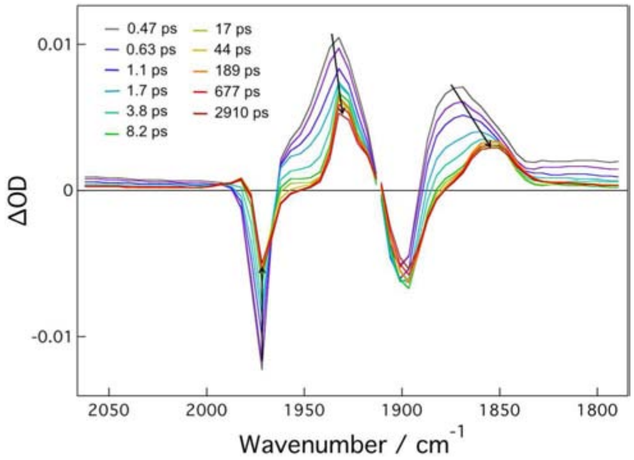

Figure 5. fs-TRIR spectra of **II** in THF, λ_{ex} = 675 nm.

The spectra of the molybdenum complex **I** in CH_2Cl_2 with excitation at 514 nm (Figure 6) are somewhat different from the tungsten analog, though the ground-state bleaches at 1975 and 1905 cm^{-1} again correspond quite well to the 'A' and 'E' CO stretches in the ground-state molecule. There are, however, new IR bands shifted to both higher and lower energy associated with the singlet state (1996, 1933, and 1870 cm^{-1}), which decay to longer-lived triplet state vibrations solely at higher energy relative to the ground state (1984 and 1919 cm^{-1}).

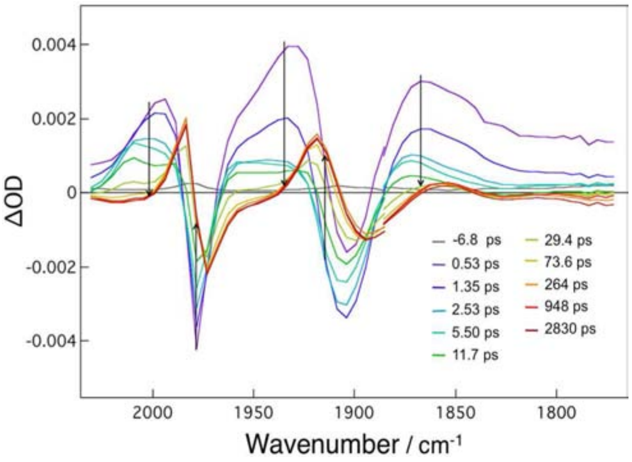

Figure 6. fs-TRIR spectra of **I** in CH_2Cl_2, λ_{ex} = 514 nm.

Clearly, the nature of the triplet state is different between the two complexes. In the tungsten case, the shift of $\nu(CO)$ to lower energy relative to both the ground and S_1 states is consistent with T_1 being ^{3}MLCT, and furthermore this state has charge more concentrated on the arene $Cr(CO)_3$ unit(s). For the molybdenum complex, the long-lived T_1 state IR bands at ~10 cm^{-1} higher energy relative to the ground state are readily rationalized by this state instead being ^{3}MoMo$\delta\delta^*$. The removal of an electron from the δ orbital reduces the $Mo_2\delta$ to benzoate backbonding, inductively reducing the backbonding to CO π^*. Note, the ground-state absorptions for both **I** and **II** are considerably lower than those for $(\eta^6\text{-}C_6H_5CO_2Me)Cr(CO)_3$ and those for **II** are lower than **I**, demonstrating the correlation of the vibrational energy with the amount of $M_2\delta$ to benzoate backbonding. The higher values of $\nu(CO)$ for the T_1 state in **I** are in remarkably good agreement with the triplet-state calculation performed on **I′**, which gives a ^{3}MoMo$\delta\delta^*$ state with $\nu(CO)$ bands to higher energy by ~10 cm^{-1}. Though the calculations on the model complex **II′** also predict a ^{3}WW$\delta\delta^*$ state with a shift to higher energy of 8 cm^{-1}, the fs-TRIR spectra instead reveal $\nu(CO)$ shifts to lower energy, further supporting the assignment of the T_1 state for **II** as ^{3}MLCT.

Before further discussion of the excited-state spectra, it should be noted that both compounds are being excited into the lowest energy electronic absorptions. Based on the calculations and knowledge of the relative energies of the $M_2\delta$ orbitals, it is clear that there is a greater mixing in the HOMO of the $Mo_2\delta$ and Cr t_{2g} orbitals than for $W_2\delta$. In an earlier work, George and co-workers examined the TRIR spectra of a methyl benzoate chromium tricarbonyl complex. With excitation at 400 nm they also observed excited IR bands to both higher and lower energy relative to a ground-state $\nu(CO)$ vibration. They assigned this to the excitation of both MLCT transitions, namely Cr d_π to CO π^* and Cr d_π to benzoate π^*. The former reduces the C−O bond order and shifts the vibration to lower energy, while the latter removes an electron from the t_{2g} orbitals, reducing the Cr−CO back bonding and thus yields a shift of $\nu(CO)$ to higher energy.[27] It seems reasonable in the case of compound **I** to invoke a somewhat related argument, namely that $M_2\delta$ to benzoate charge transfer will lead to enhanced Cr t_{tg}^6 to CO π^* back bonding and thus a shift to lower energy, while a Cr d_π to arene π^* charge transfer will increase ν(CO). Due to the enhanced mixing with the Cr t_{2g} orbitals, it is believed that the lowest energy transition contains a mixture of $Mo_2\delta$ and Cr d_π to benzoate π^* leading to the more complicated spectra. In compound **II** with a higher energy $W_2\delta$ orbital and lower energy ^{1}MLCT, the situation is clearer in that we only see ν(CO) shift to lower energy, consistent with only $M_2\delta$ to benzoate π^* charge transfer as predicted by the calculations. As stated previously, however, there is still slight involvement of chromium orbitals in the transition evidenced by the T_1 transient bands positioned to higher energy.

The next question to be addressed is whether the MLCT states are localized on one benzoate chromium tricarbonyl unit or delocalized over both. To our knowledge there are no IR characterized benzoate chromium tricarbonyl anions of the type $(\eta^6\text{-}C_6H_5CO_2Me)Cr(CO)_3^-$, so infrared data on the ^{1}MLCT states of the present compounds are best compared to predictions based on DFT calculations for $(\eta^6\text{-}C_6H_5CO_2H)Cr(CO)_3^-$ and the anions *trans*-$M_2(O_2CH)_2[O_2CC_6H_5\text{-}\eta^6\text{-}Cr(CO)_3]_2^-$. Comparisons are made with the anions because it is well-known that the spectral features of ligands in MLCT states resemble those of the reduced ligand.

Table 1 summarizes the calculated ν(CO) values for the carbonyl ligands in $(\eta^6\text{-}C_6H_5CO_2H)Cr(CO)_3$ and its anion along with those for the model compounds of **I′** and **II′** and their respective anions. In the calculations of the anions $[\mathbf{I}']^-$ and $[\mathbf{II}']^-$, the molecular orbital description yields a delocalized charge over the whole molecule but more specifically over the two ligands that contribute to the LUMO, namely the *trans*-$(O_2C\text{-}\eta^6\text{-}C_6H_5)Cr(CO)_3$ moieties. For the $(\eta^6\text{-}C_6H_5CO_2H)Cr(CO)_3$ molecule, reduction shifts the 'A' band by 70 cm^{-1} and those derived from the formal 'E' mode by 88 and 96 cm^{-1}. The calculations of the model compounds **I′** and **II′** and their respective anions show a smaller shift ranging from 48 to 53 cm^{-1}, almost half the magnitude for the mononuclear chromium anion.

The experimental shift of the carbonyl ν(CO) bands based on fs-TRIR for the complexes **I** and **II** is still smaller than those predicted for the model compounds falling in the range 25−35 cm^{-1} (Table 2). Bearing in mind the approximation being made, namely that the IR data for the ^{1}MLCT state should resemble that of the anion, the observed data correspond rather well to that of a delocalized ^{1}MLCT state. That is to say that the negative charge resides on both *trans*-$(O_2C\text{-}\eta^6\text{-}C_6H_5)Cr(CO)_3$ units and is not localized on just one.

Table 2. Experimental Ground and Excited State ν(CO) Wavenumbers of I and II, Measured in THF

	I		II	
	'A'	'E'	'A'	'E'
ground state	1977	1908	1971	1903
^{1}Cr-LCT	1996	1933	–	–
$^1M_2$-LCT	1933	1870	1935	1873
triplet state	1984	1919	1930	1853

2.8. Photodissociative Properties of I in THF.

The initial study of **I** was performed in THF and yielded puzzling results. The fs-TRIR spectra recorded in THF in the carbonyl stretching region are shown in Figure 7. The first striking feature is the appearance of two IR bleaches ~1900 and 1840 cm^{-1} which do not correspond to ground-state bleaches but rather are assigned to an efficiently formed photoproduct. These persist at long reaction times (>3 ns), as do IR absorptions to higher energies (1920 and 1865 cm^{-1}) assignable to a T_1 state. It is appropriate to note that the spectra shown in Figure 7 were obtained from a stationary cell. When the sample was moved manually during the fs-TRIR experiment (Figure 8), the spectra were essentially the sum of those shown in Figures 6 and 7.

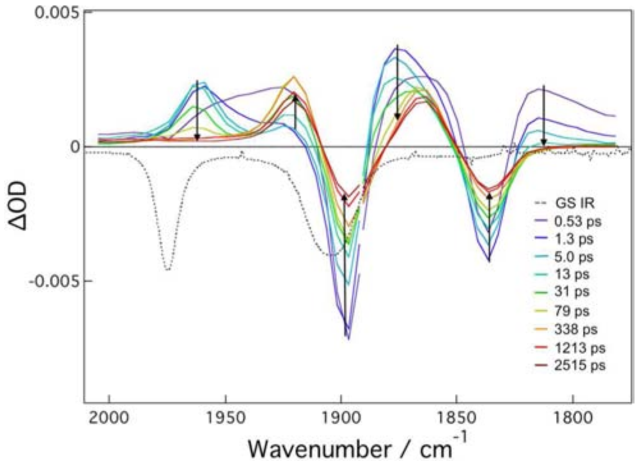

Figure 7. fs-TRIR spectra of **I** in THF, λ_{ex} = 514 nm.

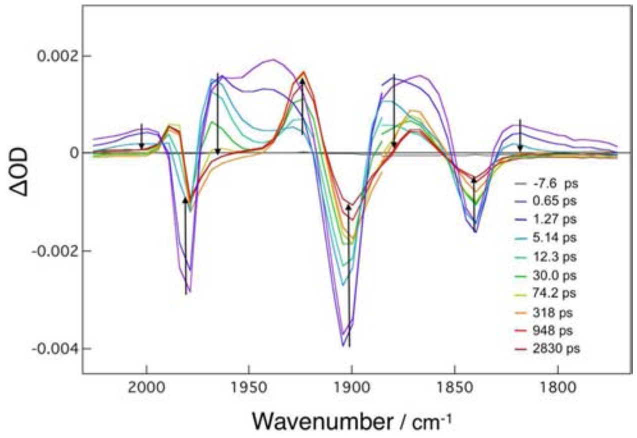

Figure 8. fs-TRIR spectra of **I** in THF with manual translation, λ_{ex} = 514 nm.

To gain further information on the photoproduct, a steady-state photolysis experiment was performed on a sample of **I** in THF (Figure S5). Almost immediately, a decrease in intensity of the 'A' band at 1977 cm^{-1} and the growth of a new band at 1840 cm^{-1} was observed. The IR band at ~1900 cm^{-1} shows a narrowing and shift to slightly lower energy. Upon ceasing photolysis, the new IR bands decrease in intensity over the course of hours, indicating a reversible or at least quasi-reversible process.

We cannot fully explain these observations at this time, but note that they most likely correspond to a reversible dissociation of a CO ligand in the donor solvent THF. This hypothesis is supported by the new vibrations closely matching those of a $(\eta^6\text{-}C_6H_6)Cr(CO)_2(DHF)$ species (DHF = dihydrofuran).[33] Also, in previous time-resolved studies of

(η^6-$C_6H_5CO_2Me$)$Cr(CO)_3$, George and co-workers found that excitation at 400 nm generates both metal-to-arene charge transfer (MACT) and metal-to-carbonyl charge transfer (MCCT) states. As the MCCT state decays, formation of a CO-loss product is observed with new ν(CO) bands shifted ~50 cm^{-1} to lower energy from the ground state. The similar effect seen for compound **I** with excitation at 514 nm could be ascribed to the involvement of Cr t_{2g} to benzoate π^* transitions in the S_1 state, which would leave a partial hole on the chromium and thus weaken the Cr−C bond. Interestingly, a coordinating solvent, such as THF, appears necessary to facilitate photoproduct formation, while this was not the case for the methyl benzoate complex. Lower energy excitation (λ_{ex} = 575 nm) still led to photoproduct formation though it was slowed considerably due to the weaker absorption at that wavelength, injection of less excess vibrational energy, or a combination of both.

Though not noticeable in the TRIR spectra of **II**, the compound also shows evidence of photoproduct formation with prolonged excitation at 675 nm. However, the species is formed much less efficiently and is shorter lived, possibly due to decomposition of the product (Figure S6). This indicates there is still some degree of chromium character in the HOMO of **II**, though the overlap is weaker. In the case of both complexes, it appears possible to effect ligand loss with much lower excitation energies than has been previously observed for chromium half-sandwich compounds. The full characterization of the photoproduct and its dynamics are the subject of a continuing investigation.

3. CONCLUSION

The attachment of a benzoate chromium tricarbonyl unit to dimolybdenum and ditungsten quadruply bonded centers has provided a convenient spectroscopic probe for studies of MLCT states in a molecular triad. The electronic structure calculations reveal that when M = Mo, the HOMO, though primarily the $Mo_2\delta$ orbital, has a significant component of a chromium t_{2g}-based orbital. This orbital is the Cr dπ orbital which has δ symmetry with respect to the arene ring. For both complexes **I** and **II**, the lowest energy electronic transition is $M_2\delta$ to benzoate π^*. In the case of M = Mo, this transition also has some Cr d_π to arene π^* contribution, potentially facilitating CO dissociation in THF solvent.

The fs-TRIR spectra for the molybdenum complex in CH_2Cl_2 more closely resemble that of the tungsten complex in not being accompanied by a photodissociation, and for both complexes we are able to examine the nature of the singlet and triplet states. For molybdenum the triplet state is $^3MoMo\delta\delta^*$, and this can be claimed with certainty based on both the long lifetime (24 μs) and the emission at ~1100 nm which shows vibronic features associated with ν(MoMo). It is, however, most interesting that the T_1 state for the molybdenum complex shows significant transient signals for the $Cr(CO)_3$ unit with a slight shift to higher ν(CO) values due to removal of an electron from the HOMO with Cr and Mo character.

In the case of tungsten, the lower energy of the $W_2\delta$ to benzoate π^* transition leads to S_1 and T_1 MLCT states. There is again, however, a detectible difference in ν(CO) of the $Cr(CO)_3$ unit in each state. For both S_1 and T_1, ν(CO) shift to lower energy is consistent with negative charge being placed on the benzoate ligands. There is evidence of some chromium character in the T_1 state, possibly due to the triplet state being more concentrated on the (η^6-$C_6H_5CO_2$)$Cr(CO)_3$ portion. For the S_1 states of both metal complexes, the shift in ν(CO) relative to the ground state is suggestive of charge delocalized over both (η^6-$C_6H_5CO_2$)$Cr(CO)_3$ units.

In contrast to the extensive studies of metal carbonyl complexes, this is, to our knowledge, the first study in which the carbonyl groups have been monitored in both singlet and triplet excited states. The rich photophysical properties of these complexes and the wide variety of other carbonyl complexes available make triads of this type interesting subjects for future study.

■ ASSOCIATED CONTENT

Ⓢ Supporting Information

Materials and methods, synthesis, and characterization of **I** and **II**; crystallographic information, emission spectra, fs- and ns-TA spectra, and steady-state irradiation data for **I**; orbital energy diagram, fs-TA and fs-TRIR spectra (λ_{ex} = 514 nm) for **II**. This material is available free of charge via the Internet at http://pubs.acs.org.

■ AUTHOR INFORMATION

Corresponding Author

Chisholm@chemistry.ohio-state.edu

Notes

The authors declare no competing financial interest.

■ ACKNOWLEDGMENTS

The authors acknowledge Dr. Judith Gallucci for collection of the single crystal X-ray data and Dr. Claudia Turro for use of instrumentation. This work was supported by the NSF grant CHE-0957191 and the OSU Institute for Materials Research. Computational resources were provided by the Ohio Supercomputing Center. S.E.B. acknowledges support from the National Defense Science and Engineering Graduate (NDSEG) Fellowship.

■ REFERENCES

(1) Hopkins, M. D.; Gray, H. B.; Miskowski, V. M. *Polyhedron* **1987**, *6*, 705−714.

(2) Miskowski, V. M.; Goldbeck, R. A.; Kliger, D. S.; Gray, H. B. *Inorg. Chem.* **1979**, *18*, 86−89.

(3) Byrnes, M. J.; Chisholm, M. H.; Clark, R. J. H.; Gallucci, J. C.; Hadad, C. M.; Patmore, N. J. *Inorg. Chem.* **2004**, *43*, 6334−6344.

(4) Cotton, F. A.; Murillo, C. A.; Walton, R. A. *Multiple Bonds Between Metal Atoms*; 3rd ed.; Springer Science: Berlin, Germany, 2005.

(5) Byrnes, M. J.; Chisholm, M. H.; Gallucci, J. C.; Liu, Y.; Ramnauth, R.; Turro, C. *J. Am. Chem. Soc.* **2005**, *127*, 17343−17352.

(6) Chisholm, M. H.; Chou, P.-T.; Chou, Y.-H.; Ghosh, Y.; Gustafson, T. L.; Ho, M.-L. *Inorg. Chem.* **2008**, *47*, 3415−3425.

(7) Alberding, B. G.; Chisholm, M. H.; Chou, Y.-H.; Ghosh, Y.; Gustafson, T. L.; Liu, Y.; Turro, C. *Inorg. Chem.* **2009**, *48*, 11187−11195.

(8) Alberding, B. G.; Chisholm, M. H.; Gallucci, J. C.; Ghosh, Y.; Gustafson, T. L. *Proc. Natl. Acad. Sci. U.S.A.* **2011**, *108*, 8152−8156.

(9) Brown, D. J.; Chisholm, M. H.; Gallucci, J. C. *Dalton Trans.* **2008**, 1615−1624.

(10) Schoonover, J. R.; Strouse, G. F. *Chem. Rev.* **1998**, *98*, 1335−1355.

(11) McFarlane, K.; Lee, B.; Bridgewater, J.; Ford, P. C. *J. Organomet. Chem.* **1998**, *554*, 49−61.

(12) George, M. W.; Turner, J. J. *Coord. Chem. Rev.* **1998**, *177*, 201−217.

(13) Busby, M.; Matousek, P.; Towrie, M.; Clark, I. P.; Motevalli, M.; Hartl, F.; Vicek, A. *Inorg. Chem.* **2004**, *43*, 4523−4530.

(14) Liard, D. J.; Busby, M.; Matousek, P.; Towrie, M.; Vlcek, A. *J. Phys. Chem. A* **2004**, *108*, 2363−2369.
(15) Chong, T. S.; Li, P.; Leong, W. K.; Fan, W. Y. *J. Organomet. Chem.* **2005**, *690*, 4132−4138.
(16) Gabrielsson, A.; Hartl, F.; Zhang, H.; Smith, J. R. L.; Towrie, M.; Vlcek, A.; Perutz, R. N. *J. Am. Chem. Soc.* **2006**, *128*, 4253−4266.
(17) Polo, A. S.; Itokazu, M. K.; Frin, K. M.; Patrocinio, A. O. D.; Iha, N. Y. M. *Coord. Chem. Rev.* **2006**, *250*, 1669−1680.
(18) Vlcek, A.; Busby, M. *Coord. Chem. Rev.* **2006**, *250*, 1755−1762.
(19) Butler, J. M.; George, M. W.; Schoonover, J. R.; Dattelbaum, D. M.; Meyer, T. J. *Coord. Chem. Rev.* **2007**, *251*, 492−514.
(20) Li, G.; Parimal, K.; Vyas, S.; Hadad, C. M.; Flood, A. H.; Glusac, K. D. *J. Am. Chem. Soc.* **2009**, *131*, 11656−11702.
(21) El Nahhas, A.; Consani, C.; Blanco-Rodriguez, A. M.; Lancaster, K. M.; Braem, O.; Cannizzo, A.; Towrie, M.; Clark, I. P.; Zalis, S.; Chergui, M.; Vlcek, A. *Inorg. Chem.* **2011**, *50*, 2932−2943.
(22) Yarnell, J. E.; Deaton, J. C.; McCusker, C. E.; Castellano, F. *Inorg. Chem.* **2011**, *50*, 7820−7830.
(23) George, M. W.; Long, C.; Pryce, M. T.; Sun, X.-Z.; Vuong, K. Q. *Organometallics* **2012**, *31*, 268−272.
(24) Creaven, B. S.; George, M. W.; Ginzburg, A. G.; Hughes, C.; Kelly, J. M.; Long, C.; McGrath, I. M.; Pryce, M. T. *Organometallics* **1993**, *12*, 3127−3131.
(25) Alamiry, M. A. H.; Boyle, N. M.; Brookes, C. M.; George, M. W.; Long, C.; Portius, P.; Pryce, M. T.; Ronayne, K. L.; Sun, X.-Z.; Towrie, M.; Vuong, K. Q. *Organometallics* **2009**, *28*, 1461−1468.
(26) Clark, I. P.; George, M. W.; Greetham, G. M.; Harvey, E. C.; Long, C.; Manton, J. C.; Pryce, M. T. *J. Phys. Chem. A* **2010**, *114*, 11425−11431.
(27) Clark, I. P.; George, M. W.; Greetham, G. M.; Harvey, E. C.; Long, C.; Manton, J. C.; Pryce, M. T. *J. Phys. Chem. A* **2011**, *115*, 2985−2993.
(28) Long, C. *J. Phys. Chem. A* **2012**, *116*, 6845−6850.
(29) Brammer, L.; Rivas, J. C. M.; Atencio, R.; Fang, S.; Pigge, F. C. *J. Chem. Soc., Dalton Trans.* **2000**, 3855−3867.
(30) Chisholm, M. H.; Epstein, A. J.; Gallucci, J. C.; Feil, F.; Pirkle, W. *Angew. Chem., Int. Ed.* **2005**, *44*, 6537−6540.
(31) Djukic, J.-P.; Rose-Munch, F.; Rose, E. *Eur. J. Inorg. Chem.* **2000**, *2000*, 1295−1306.
(32) Chisholm, M. H.; Gustafson, T. L.; Turro, C. *Acc. Chem. Res.* **2012**, DOI: 10.1021/ar3002206.
(33) Bengali, A. A.; Hall, M. B.; Wu, H. *Organometallics* **2008**, *27*, 5826−5829.